Evaluation of the onset of green-up in temperate deciduous broadleaf forests derived from Moderate Resolution Imaging Spectroradiometer (MODIS) data

Kamel Soudani [a,*], Guerric le Maire [a], Eric Dufrêne [a], Christophe François [a], Nicolas Delpierre [a], Erwin Ulrich [b], Sébastien Cecchini [b]

[a] *Univ Paris-Sud, Laboratoire Ecologie Systématique et Evolution, UMR8079, Orsay, F-91405; CNRS, Orsay, F-91405; AgroParisTech, Paris, F-75231, France*
[b] *Office National des Forêts, Département Recherche, Boulevard de Constance, 77300 Fontainebleau, France*

Abstract

Vegetation phenology is the chronology of periodic phases of development. It constitutes an efficient bio-indicator of impacts of climate changes and a key parameter for understanding and modelling vegetation-climate interactions and their implications on carbon cycling. Numerous studies were devoted to the remote sensing of vegetation phenology. Most of these were carried out using data acquired by AVHRR instrument onboard NOAA meteorological satellites. Since 1999, multispectral images were acquired over the whole earth surface every one to two days by MODIS instrument onboard Terra and Aqua platforms. In comparison with AVHRR, MODIS constitutes a significant technical improvement in terms of spatial resolution, spectral resolution, geolocation accuracy, atmospheric corrections scheme and cloud screening and sensor calibration. In this study, 250 m daily MODIS data were used to derive precise vegetation phenological dates over deciduous forest stands. Phenological markers derived from MODIS time-series and provided by MODIS Global Land Cover Dynamics product (MOD12Q2) were compared to field measurements carried out over the main deciduous forest stands across France and over five years. We show that the inflexion point of the asymmetric double-sigmoid function fitted to NDVI temporal profile is a good marker of the onset of green-up in deciduous stands. At plot level, the prediction uncertainty is 8.5 days and the bias is 3.5 days. MODIS Global Land Cover Dynamics MOD12Q2 provides estimates of onset of green-up dates which deviate substantially from *in situ* observations and do not perform better than the null model. RMSE values are 20.5 days (bias -17 days) using the onset of greenness increase and 36.5 days (bias 34.5 days) using the onset of greenness maximum. An improvement of prediction quality is obtained if we consider the average of MOD12Q2 onset of greenness increase and maximum as marker of onset of green-up date. RMSE decreases to 16.5 days and bias to 7.5 days.
© 2008 Elsevier Inc. All rights reserved.

Keywords: Forest phenology; MODIS; NDVI time-series; MOD12Q2

1. Introduction

Phenology is the chronology of periodic phases of development of living species. For vegetation ecosystems, phenology characterises the seasonal behaviour of the main biological events such as budburst, flowering, fructification and leaf senescence. The vegetation seasonality reflects adaptive responses of species to climate variability, mainly the temperature and daylength in temperate and boreal regions (Kramer et al., 2000) and water availability in arid and semi-arid regions (Zhang et al., 2005). Therefore, timing of phenological cycles is used as an efficient bio-indicator of climate change impacts (Menzel, 2002; Chuine et al., 2004; Clark and Thompson, 2004) and as a key parameter for understanding and modelling vegetation–climate interactions (Crucifix et al., 2005) and their implications on carbon cycling (Kaduk and Heimann, 1996). *In situ* observations (national phenological networks, phenological gardens, GLOBE student observations, etc.), empirical or bioclimatic

---

models (Schwartz, 1990; Schaber and Badeck, 2003) and remote sensing constitute the three possible ways for monitoring the timing of vegetation phenological events. Ground based observations of vegetation phenology across large areas are expensive, time consuming and subject to uncertainty due to operator bias. Empirical and bioclimatic models are often species specific and calibrated at local scales (Chuine et al., 2000). Their application at global scale may not be accurate and depends also on availability of vegetation maps and complete and consistent climate records used as forcing variables. Remote sensing has the advantages of being the only way of sampling at low-cost with good temporal repeatability over large and inaccessible regions.

Numerous studies were devoted to the remote sensing of vegetation phenology. These studies, mainly using NOAA AVHRR data, focused in two general issues: (1) developing methods for reconstructing a good quality satellite time-series datasets (Holben, 1986; Viovy et al., 1992; Cihlar et al., 1998; Jönsson and Eklundh, 2002; Chen et al., 2004); and (2) exploring and evaluating the use of satellite derived phenological metrics for studying terrestrial ecosystems dynamics at different spatial and temporal scales (Myneni et al., 1997; Schwartz et al., 2002; White et al., 2002; Stöckli and Vidale, 2004; Fisher et al., 2006).

Generally speaking, remote sensing of key dates of main phenological events was based on tracking significant changes on temporal trajectories of spectral vegetation indices (SVIs) which are more stable over time than single bands. That requires SVI time-series with good time resolution, over homogeneous area, cloud-free and not affected by atmospheric and geometric effects and variations in sensor characteristics (calibration, spectral responses). Cloud cover is the most serious problem in optical remote sensing of earth's surface. Numerous techniques were developed in order to automatically retain cloud-free images. The most commonly used method is the Maximum Value Composite technique MVC developed by Holben (1986) which produces composite image over a fixed period of time by retaining for each pixel the maximum NDVI value from daily images acquired over this period. Because this method suffers a number of drawbacks particularly a preferential selection of off-nadir values (Lovell et al., 2003), a modified version of MVC method by selecting maximum SVI value with view zenith angles closest to nadir view is used in generating MODIS SVI products (Wolfe et al., 1998). Despite this continuous technical improvement, satellite data are not completely "clean" but contain residual effects due to sub-pixel clouds, cloud shadows and haze (Cihlar et al., 1998). Other methods for filtering cloud cover and noise removing were also proposed such as Best Index Slope Extraction (BISE) (Viovy et al., 1992), function fitting (Jönsson and Eklundh, 2002; Zhang et al., 2003), Fourier analysis (Wagenseil and Samimi, 2006; Moody and Johnson, 2001), Savitsky–Golay filter (Chen et al., 2004) and mean value iteration filter (Ma and Veroustaete, 2006).

Considerable effort has also been spent in the last decade on development of methods for identifying and calculating phenological transition dates using SVI time-series. Briefly, these methods can be categorized as follows: (1) Using a user-defined threshold separating growing season from dormancy period.

The threshold is fixed at single value depending on vegetation type or defined at pixel level (White et al., 1997; Schwartz et al., 2002; White et al., 2002; Suzuki et al., 2003; Chen et al., 2004; White and Nemani, 2006; Delbart et al., 2006; Studer et al., 2007); (2) Using numerical procedures to detect the period showing significant and rapid increase in SVI time-series (Kaduk and Heimann, 1996; Moulin et al., 1997; Schwartz et al., 2002) and (3) Using the parameters of appropriate functions fitted to SVI time-series (Jönsson and Eklundh, 2002; Zhang et al., 2003; Fisher et al., 2006; Beck et al., 2006).

Over deciduous broadleaf stands, Schwartz et al. (2002) derived the dates of onset of greenness from NOAA AVHRR using two methods, one based on a site-specific NDVI time-constant threshold (White et al., 1997; White et al., 1999) fixed using a historical analysis and the other based on rapid increase of NDVI within an average delayed moving window (Reed et al., 1994). Results showed that the both methods allow detecting annual variations of dates of onset of greenness with moderate accuracy. Similar methods were also used in Studer et al. (2007) to assess the impacts of climate variability on vegetation phenology who found significant links between temperature anomalies and phenological metrics derived from NOAA AVHRR time-series and from ground observations. Despite the good agreement between predictions and observations, these methods are known to be sensitive to noise and gaps in SVI time-series (Jenkins et al., 2002). Also as underlined in Zhang et al. (2003), they are not applicable over ecosystems characterised by multiple growth and senescence cycles. More recently, Zhang et al. (2003) represented vegetation phenology by a series of piecewise logistic functions of time. Fisher et al. (2006), Ahl et al. (2006) and Fisher and Mustard (2007) used Zhang's method to predict the timings of onset of greenness over deciduous broadleaf forests. In Ahl et al. (2006), several standard MODIS products with different spatial and temporal resolutions were used. The best agreement between predictions and field observations was found using daily MODIS NDVI (within 1 day). Using 16 days composite MODIS SVI products, discrepancy between field observations and predictions was more than 12 days. The authors suggested that the effects of understory and the temporal compositing MODIS data are the main factors explaining this discrepancy. Fisher et al. (2006) and Fisher and Mustard (2007) modified Zhang's method and represented phenology by a unique double-sigmoid function over deciduous forests characterized by two single growth and senescence periods. The authors also analyzed uncertainties of the fitted parameters and concluded that this representation responds well to seasonal vegetation changes and is highly robust to noise and sparse data during the transition seasons.

As underlined above, the most of studies were carried out using NOAA AVHRR data onboard meteorological satellites. In comparison with AVHRR, MODIS constitutes a significant improvement in terms of spatial resolution (250 m to 1 km vs 1 km), spectral resolution (36 spectral bands vs 6), geolocation accuracy [<50 m at nadir (Wolfe et al., 2002) vs 1 to 2 km (Box et al., 2006)], atmospheric corrections scheme and cloud screening (Heidinger et al., 2002) and sensor calibration (Justice et al., 1998). Images acquired by MODIS are routinely

used to derive global products for monitoring and studying land surface changes at different time steps. The last product generated from MODIS reflectance measurements is the land cover dynamics (MOD12Q2) which gives estimates of the timings of vegetation phenology at global scale with 1 km^2 spatial resolution. MOD12Q2 phenology, like other MODIS products, is produced according to a well documented scheme and the validation process of this product is currently underway (Zhang et al., 2006).

In this study, MODIS based phenological markers were compared to field measurements carried out over homogeneous forest stands across France and over five years. More precisely, the main objectives are: (1) to develop a method using 250 m daily MODIS NDVI time-series to estimate the date of the onset of green-up of main deciduous forest species in France; (2) to compare these estimates with the phenological observations carried out within the French RENECOFOR network (National network for Long-Term Monitoring of Forest Ecosystems) and (3) to evaluate the vegetation phenological markers provided by MODIS Global Land Cover Dynamics product (MOD12Q2).

2. Materials and methods

2.1. Study sites

The study sites are located between latitudes 42°55′53″ N and 50°10′16″ N and between longitudes 3°32′34″ W and 7°43′46″E and belong to the French RENECOFOR network (see http://www.onf.fr/pro/Renecofor/Placettes.htm). The French RENECOFOR network was created in 1992 by the French National Forest Service (Office National des Forêts) and consists of 102 deciduous and evergreen permanent plots of a homogenous area of 2 ha each. The main objectives are documenting and monitoring long-term changes in state of health, growth and biochemical cycles of carbon and minerals nutrients of the more representative forest ecosystems in France. The phenological database of RENECOFOR network provides the more complete set of phenological observations in natural conditions of main forest ecosystems in Metropolitan France in terms of species, geographic and climate distribution (Fig. 1). All climatic conditions are represented by RENECOFOR stands. Briefly, climate is mainly temperate but four climate types may be distinguished: oceanic along the west coast and in the north, continental in the interior of the country at mid-latitudes, Mediterranean in the south along the Mediterranean coast and mountain at high elevations where snow precipitations are frequent in winter.

This study focuses on the main deciduous forest ecosystems belonging to RENECOFOR network. Field observations were carried out over 50 permanent plots representative of pure and homogeneous deciduous forest stands managed by the National French Forest Service. These stands are divided as follows: 9 plots of pedunculate oak (Quercus robur (Matus) Liebl), 19 plots of sessile oak (Quercus petraea (Matus) Liebl), 2 plots of a mixture of the two oak species, and 20 plots of European beech (Fagus sylvatica, L.). Stands are mostly managed as pure and even-aged high forests in which trees of the main overstory are in the same age class. The average age of plots ranges between 60 and 120 years. Average elevation (asl) is 200 m in oak plots (20–370 m) and 560 m in beech plots (50–1400 m). Average topography is gentle to flat of about 11% in beech plots and 3% in oak plots (Table 1).

2.2. Data

2.2.1. In situ phenological observations

In situ phenological observations used in this study were carried out over a period of five years, from 2000 to 2004. In each plot, 36 trees were chosen and numbered. All these trees are located in a fenced part of 0.5 ha located in the centre of the plot. These trees are representative of the plot in terms of species, age and structure. At each year, phenological observations were
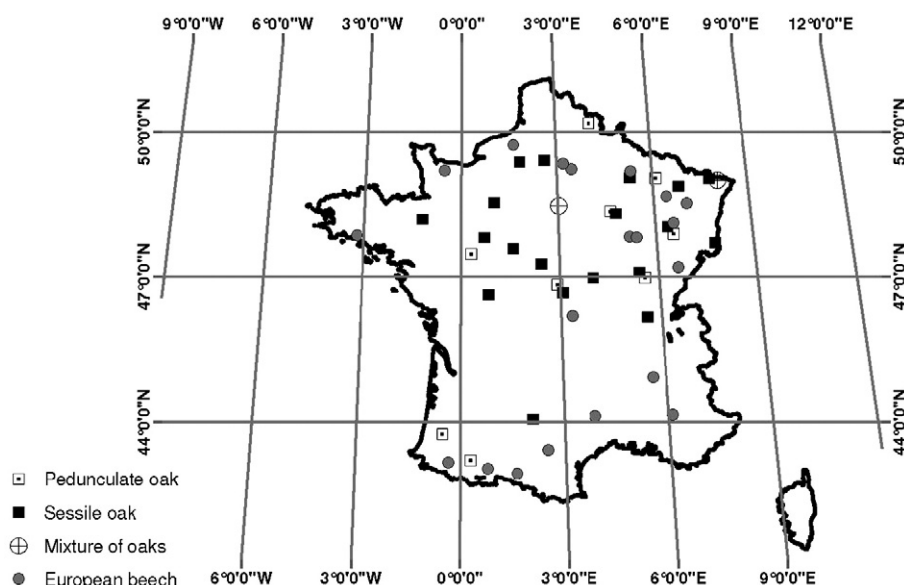

Fig. 1. Geographic locations of RENECOFOR deciduous broadleaf forest stands.

Table 1
Geographic locations and main characteristics of RENECOFOR deciduous broadleaf forest stands

Plot name	Longitude (°)	Latitude (°)	Stand structure	Main overstory specie	Elevation (m)	Slope (%)	Orientation
O1	4.30408	48.34608	coppice-with-standards	Pedunculate oak	115	0	Flat
O2	2.57264	46.82518	high forest	Pedunculate oak	175	2	NW
O3	−0.84340	43.73577	high forest	Pedunculate oak	20	5	NE
O4	−0.03240	47.45490	high forest	Pedunculate oak	57	0	SW
O5	5.76569	49.02131	coppice-with-standards	Pedunculate oak	220	0	Flat
O6	3.75356	50.17056	high forest	Pedunculate oak	149	3	Flat
O7	−0.03912	43.20230	high forest	Pedunculate oak	370	12	SE
O8	6.21130	47.87029	high forest	Pedunculate oak	240	0	Flat
O9	5.24288	46.96929	high forest	Pedunculate oak	190	0	Flat
S1	5.23795	46.17013	high forest	Sessile oak	260	3	Flat
S2	2.72579	46.66690	high forest	Sessile oak	260	0	Flat
S3	4.46106	48.29758	high forest	Sessile oak	160	0	Flat
S4	2.12500	47.25352	high forest	Sessile oak	176	1	Flat
S5	5.07479	47.08163	high forest	Sessile oak	220	0	flat
S6	1.50183	49.36483	high forest	Sessile oak	175	0	Flat
S7	−1.53558	48.17706	high forest	Sessile oak	80	0	Flat
S8	1.25866	47.56857	high forest	Sessile oak	127	0	Flat
S9	4.95912	49.03213	coppice-with-standards	Sessile oak	180	2	S
S10	6.48244	48.87090	high forest	Sessile oak	315	4	NE
S11	7.46088	49.01554	high forest	Sessile oak	320	15	NW
S12	3.66001	46.96956	high forest	Sessile oak	270	7	SW
S13	2.29699	49.39411	high forest	Sessile oak	55	1	Flat
S14	0.67861	48.52232	high forest	Sessile oak	220	5	SE
S15	7.46621	47.69304	coppice-with-standards	Sessile oak	256	0	Flat
S16	0.37903	47.79560	high forest	Sessile oak	170	0	Flat
S17	1.74823	44.04490	high forest	Sessile oak	300	18	SE
S18	0.49409	46.62643	high forest	Sessile oak	116	4	NW
S19	6.03913	48.02593	high forest	Sessile oak	330	0	Flat
OS1	7.72847	48.98973	high forest	Mixture of oaks	350	10	S
OS2	2.71650	48.45377	high forest	Mixture of oaks	80	0	Flat
H1	3.12565	49.20486	high forest	European beech	145	0	Flat
H2	2.99841	46.19265	high forest	European beech	590	15	N
H3	5.79746	44.13147	high forest	European beech	1300	50	N
H4	1.28039	42.93060	high forest	European beech	1250	32	SW
H5	−0.85788	49.18160	high forest	European beech	90	4	Flat
H6	4.85361	47.81347	high forest	European beech	400	3	NE
H7	6.27737	47.19144	high forest	European beech	570	2	W
H8	5.29446	44.91705	high forest	European beech	1320	12	W
H9	−3.54492	47.83646	high forest	European beech	50	0	Flat
H10	3.54170	44.11388	high forest	European beech	1400	25	SW
H11	5.07199	47.79476	high forest	European beech	440	0	Flat
H12	6.70539	48.50903	high forest	European beech	325	5	E
H13	6.06605	48.64812	high forest	European beech	390	2	Flat
H14	5.00361	49.17026	high forest	European beech	250	0	Flat
H15	2.87526	49.32359	high forest	European beech	138	0	Flat
H16	−0.66007	43.14926	high forest	European beech	400	44	NW
H17	0.43515	43.02562	high forest	European beech	850	25	NW
H18	1.32555	49.71038	high forest	European beech	210	0	Flat
H19	2.17690	43.41000	high forest	European beech	700	0	Flat
H20	6.24448	48.10551	high forest	European beech	400	3	W

Geographic coordinates are in WGS84.

performed a once a week on the same trees. Two dates characterising the onset of green-up were determined. These dates, termed *OG10%* and *OG90%* hereafter, were defined as the dates when 10% and 90% of the 36 trees (four and thirty two trees, respectively) have the buds open over at least 20% of the crown of each tree. Because *in situ* phenologiclal observations were carried out with one week time lag, we estimate a theoretical precision of 7 days and 3–4 days on average.

2.2.2. MODIS data and pre-processing

2.2.2.1. MODIS data. The MODIS/TERRA surface reflec- tance daily L2G global 250 m SIN grid V004 product (MOD09GQK) for years 2000–2004 and MODIS Global Land Cover Dynamics (MOD12Q2) for years 2001–2004 (2000 not available) were obtained through the Earth Observing System Data Gateway.

MOD09GQK product contains data acquired in the bands 1 (red: 620–670 nm) and 2 (near infrared: 841–876 nm) of MODIS/Terra with 250 m spatial resolution. Data were already atmospherically corrected of effects of gases, aerosols and thin cirrus clouds according the MOD09 atmospheric correction scheme in Vermote and Vermeulen (1999). In addition to red and near infrared layers, MOD09GQK contains other three Science Datasets stored with MODIS products: 250 m reflectance band quality (QA), orbit and coverage and number of observations. QA corresponds to per-pixel quality assessment flags at three different levels of detail: at the level of the individual pixel, at the level of each band and each resolution, and at the level of the whole file (for more details, see http://edcdaac.usgs.gov/modis/mod09gqkv4.asp).

MOD12Q2 product provides estimates of timing of vegetation phenological transitions for 12-months period at global scale with 1 km^2 spatial resolution. In MOD12Q2 product, the phenological dates were determined using temporal profile of Enhanced Vegetation Index (EVI) computed from the 16-day bi-directional reflectance distribution function adjusted reflectance in red, near infrared and blue bands provided by MOD43B4 product following the processing scheme given in Huete et al. (2002). Briefly, for each pixel, temporal EVI profile is built using 24 months of data, 12 months of interest bracketed by six months on either side. After elimination of doubtful EVI values, EVI profile is modelled using two sigmoidal functions from which the phenological transition dates were determined following the procedure described in Zhang et al. (2003). These dates are: onset of greenness increase *OGI* (beginning of EVI increase), onset of greenness maximum *OGM* (reaching of maximum EVI plateau), onset of greenness decrease (beginning of EVI decrease), and onset of greenness minimum (reaching of EVI minimum plateau). The two first dates are considered as the date of green-up and the date of maturity when green leaf area index reaches the maximum, respectively (Friedl et al., 2003).

2.2.2.2. Processing. From daily MOD09GQK product, only three layers were extracted: band 1, band 2 and quality assurance (QA). Then, for each year, images of the same layer were merged. For the five years concerned by this study, a total of about 4575 images were used.

From MOD12Q2 product, four layers were extracted: onset of greenness increase, onset of greenness maximum, per-date and per-pixel quality assurance flags.

In the initial stages, a layer composed of polygons of RENECOFOR plots was created. Each polygon delimits a square having an area of nine MODIS-250 m pixels centred on the centre of the plot. In order to check the homogeneity of MODIS-250 m pixels surrounding each plot which may affect the radiometric signal and alter the quality of predicted dates of phenological transitions, the polygon-based layer of plots was exported to GoogleEarth™. The composition of each pixel was described and a qualitative index of homogeneity as a form of alphabetical notation was assigned. As expected, all pixels surrounding the RENECOFOR plots belong to large forest regions and are classified by-eye as homogeneous.

2.3. Methods of detection of phenological dates from modelled Normalised Difference Vegetation Index temporal profile

MODIS red and near infrared surface reflectance and quality assurance were extracted for the central pixel of each plot. Three text files, one file for each layer, were generated and used for further processing. Fourth steps were carried out to determine the date of onset of green-up.

Firstly, reflectance in the red and near infrared bands were used to calculate the normalised difference vegetation index (NDVI) as:

$$\text{NDVI} = \frac{\text{NIR} - \text{RED}}{\text{NIR} + \text{RED}} \qquad (1)$$

We used the NDVI because it is at the native 250 m spatial resolution, given that both Red and NIR are available at 250 m. NDVI is also the most used vegetation index for a variety of vegetation remote sensing studies because it is sufficiently sensitive to capture small changes in amount of photosynthetic vegetation (Soudani et al., 2006).

Secondly, before reconstruction of NDVI temporal profiles, all spurious values were removed. In the first step, based on per-pixel QA flags, we kept only NDVI values computed using atmospherically corrected reflectance data produced at "ideal global quality". In the second step and in order to remove spurious data not flagged by QA or values showing significant deviation from their neighbours (sun and view effects, snow), a five point temporal moving window was applied. The central NDVI value of the window is compared to the average of its four neighbours. This NDVI value is removed if the absolute deviation from the average is more than 20% of the mean. The threshold of 20% was chosen after visual checking of the temporal variability of NDVI values along the temporal profile.

Thirdly, NDVI time-series for each plot and for each year was modelled by an asymmetric double-sigmoid function (ADS) using the following equation:

$$\begin{aligned} \text{NDVI}(t) = {} & (w_1 + w_2) \\ & + \frac{1}{2}(w_1 - w_2)[\tanh(w_3(t-u)) - \tanh(w_4(t-v))] \end{aligned} \qquad (2)$$

tanh is the hyperbolic tangent, *t* is the time (Day of Year) and w_1, w_2, w_3, w_4, *u*, *v* are the fitting parameters. $(w_1 + w_2)$ is the NDVI minimum in unleafy season. $(w_1 - w_2)$ is the total amplitude of NDVI temporal variations. *u* and *v* are the dates corresponding to the highest rates of change of NDVI(*t*) (maximum and minimum peaks of the first derivative of NDVI(*t*)). They are the dates of the two inflection points when the NDVI(*t*) increases during the leaf expansion (*u*) and decreases during the leaf senescence (*v*). For these two dates, NDVI(*t*) is at the middle of its amplitude. Fitting were done by minimizing the sum of squares of differences between Eq. (2) and the measured NDVI values.

Eq. (2) is based on the equation of Zhang et al. (2003) and is similar to the full equation given in Fisher et al. (2006) describing the leafy and unleafy seasons in deciduous forests. In our study, the equation of Fisher et al. has been rewritten so that

the two inflection points are directly determined by the fitting procedure. In addition, the main advantage of this rewriting is the ability to compute easily the statistical errors on the best fit parameters at the two inflections positions u and v using the Jacknife procedure (see below).

In the present study, we are interested in the date at the first inflexion point (u), used here as the main marker of the date of onset of green-up. Hereafter, we term this date *dinfNDVI*. We used the position of the inflexion point of NDVI curve because it is stable and corresponds to an advanced stage of canopy development. The positions of NDVI minimum increase and maximum were also determined following the procedure described below.

The global goodness-of-fit of the model was evaluated using Nash–Sutcliffe Efficiency E criteria (Nash and Sutcliffe, 1970).

$$E = 1 - \frac{\sum\limits_{i=1}^{N} (\mathrm{NDVI}_s - \mathrm{NDVI}_o)^2}{\sum\limits_{i=1}^{N} (\mathrm{NDVI}_o - \overline{\mathrm{NDVI}_o})^2}$$

Where NDVI_s and NDVI_o are the simulated and the observed NDVI values, respectively. N is the sample size. E may be considered as an improvement over the coefficient of determination usually used as a measure of the goodness-of-fit which is sensitive to both mean and variance of simulated data. E ranges from $-\infty$ for poor model to 1 for perfect model (Legates and McCabe, 1999).

Errors on the six fitting parameters were calculated using the jackknife procedure. The basic idea of this technique is to generate $(N+1)$ samples from one sample having N observations: N samples having $(N-1)$ observations each generated by removing in turn one observation from the initial dataset and one sample corresponding to the initial dataset. The model (Eq. (2)) was sequentially fitted using one among the $N+1$ samples. Thus, we obtain N+1 estimates of each parameter. The standard deviation of these estimates is used as a measure of the statistical precision of the parameter estimate. The standard deviation of the fitted first inflexion point of the fitted model curve was used as global quality criterion. The estimates of this parameter with a standard deviation greater than 7 days were removed from the analysis since the precision of *in situ* observations is of the same order of magnitude.

At last, in order to make the comparison possible with phenological metrics given in MOD12Q2 product, we determined the dates of the onset of NDVI increase (*dminNDVI*) and NDVI maximum (*dmaxNDVI*) (see Fig. 2 in Section 3.1). These dates are equivalent to *OGI* and *OGM* provided by MODIS MOD12Q2 product. These dates were determined analytically in MOD12Q2 product using the procedure described in Zhang et al. (2003), whereas in this study, these dates were determined numerically by finding the dates of the extrema of the B-splines fitted to the third derivative of modelled NDVI temporal profile. The different phenological markers derived from fitted NDVI time-series are illustrated in Fig. 2.

The validation of predictions obtained using NDVI fits and provided by MOD12Q2 product were done against ground-based phenological observations carried out in the RENECO-FOR Network. The statistics used are the Pearson's correlation coefficient, the root mean square error (RMSE) and the bias between predictions (P_i) and observations (O_i). The RMSE was used to evaluate the average prediction uncertainty relative to *in situ* observations:

$$\mathrm{RMSE} = \sqrt{\frac{\sum\limits_{i=1}^{N} (P_i - O_i)^2}{n}}$$

The RMSE was also compared to RMSE of the null model where the date of onset of green-up for each plot is estimated by the average of all dates over the year. RMSE > RMSE $_{\mathrm{NULL\ MODEL}}$ means that the remote sensing can not provide better predictions of phenology than taking the average of all field observations.

$$\mathrm{RMSE}_{\mathrm{NULL\ MODEL}} = \sqrt{\frac{\sum\limits_{i=1}^{N} (O_i - \overline{O})^2}{n}}$$

The bias was used to evaluate if predictions are overestimated (positive bias) or underestimated (negative bias).

$$\mathrm{Bias} = \frac{\sum\limits_{i=1}^{N} (P_i - O_i)}{n}$$

3. Results

3.1. Final dataset

From a methodological point of view, frequent gaps in NDVI data were observed (Fig. 2). These gaps were due above all to
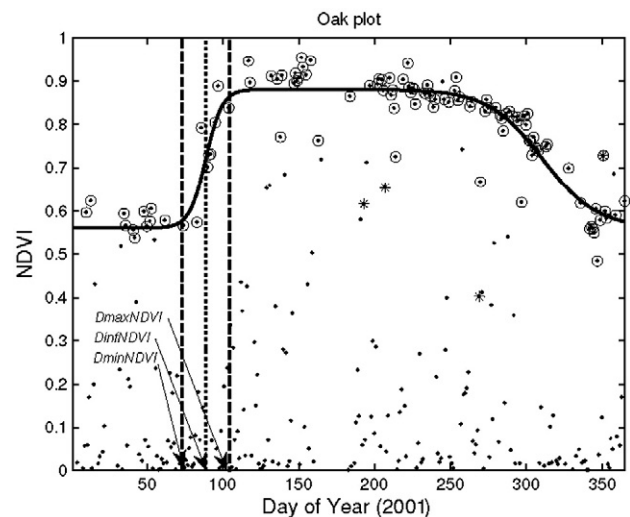

Fig. 2. Measured and fitted NDVI temporal profile over an oak stand during year 2001. (solid line): fitted asymmetric double-sigmoid function; (circle with point inside): NDVI measurements used in the fit; (stars): NDVI measurements removed using the five point moving window; (full circle): NDVI measurements removed from flags MODIS per-pixel quality assurance.
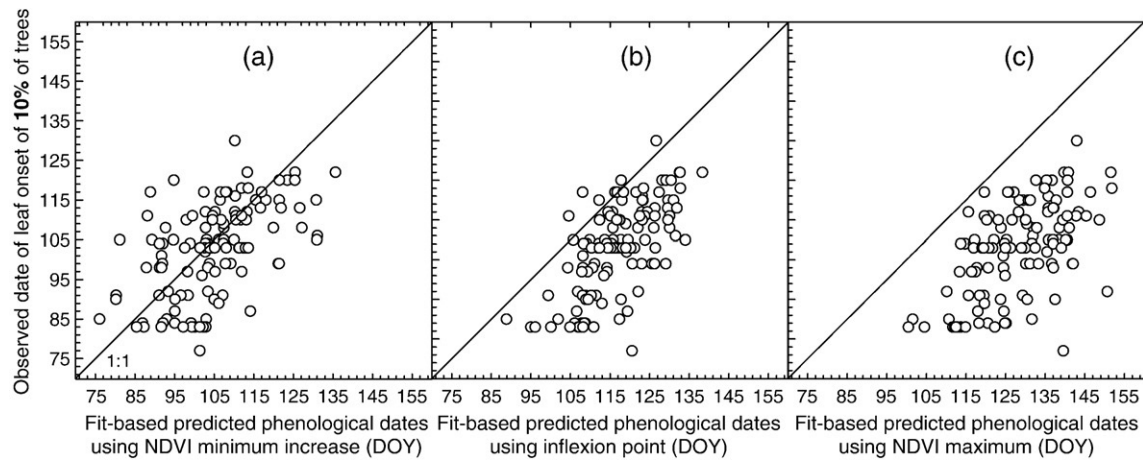
Fig. 3. Comparative analysis between predictions from fitted NDVI time-series and field observations of the date of onset of green-up at 10% (*OG10%*).

overcast conditions which are generally flagged in MODIS per-pixel quality assurance. This layer stored with MOD09 products which gives informations about the state of atmospheric corrections, clouds and other ancillary data was useful. Nevertheless, some spurious values not flagged by QA can persist and should be removed using a moving window with an appropriate length. On average over all plots, the number of days used to build NDVI temporal profiles ranges between 80 and 138 and about 109 days on average over all years. The lowest number of days is used in year 2000 and the highest in year 2003 for which heat and drought in summer were extreme in Europe. This shows that cloudy conditions may lead to serious limitations of remote sensing of phenology over many regions throughout the globe. Large time gaps in NDVI data are particularly problematic during the leaf expansion period. A small number of NDVI values over this period of time reduces the quality of the fit and increases the jackknifed standard deviation of the estimates of phenological dates. Nevertheless, the asymmetric double sigmoid function (Eq. (2)) is quite resistant to noise. Efficiency criterion ranges between 0.22 and 0.9 and the overall average is about 0.84 (not shown). Low E values do not necessarily mean that the phenological markers are misestimated because E is a global quality criterion which depends on

the scattering of data over the year. On the contrary, the jackknifed standard deviation allowed detecting phenological markers instabilities due to noise and gaps in NDVI data during the leaf expansion period. For this reason and because of gaps in MOD12Q2 product and incidental gaps in field observations, the number of plots effectively used is variable from year to year.

3.2. Comparison between in situ observations and phenological dates using fitted NDVI temporal profiles

Results of the comparative analysis between metrics based on fitted NDVI temporal profiles (*dinfNDVI*, *dminNDVI* and *dmaxNDVI*) and *in situ* observations (*OG10%* and *OG90%*) are illustrated in Figs. 3 and 4, respectively. These results are for all sites, all species and all available years. The summary statistics are given in Table 2.

In terms of prediction uncertainties, RMSE values range between 11.5 and 27.5 days by comparison with *OG10%* and between 8.5 and 18 days by comparison with *OG90%*. The lowest RMSE values are 11.5 days using *dminNDVI* and 8.5 days using *dinfNDVI* by comparison with *OG10%* and *OG90%* respectively. The lowest bias values are 2 days using
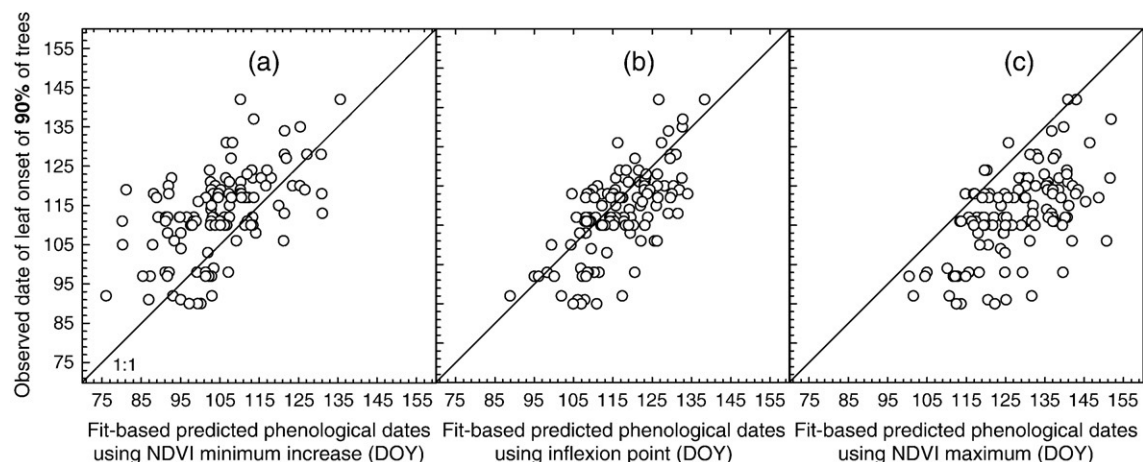

Fig. 4. Comparative analysis between predictions from fitted NDVI time-series and field observations of the date of onset of green-up at 90% (*OG90%*).

Table 2
Comparative analysis between *in situ* phenological observations *OG10%* and *OG90%* and phenological metrics derived from fitted curves on daily 250 m MODIS NDVI time-series

	Comparison with *in situ* onset of green-up *OG10%*			Comparison with *in situ* onset of green-up *OG90%*		
	dminNDVI	*dinfNDVI*	*dmaxNDVI*	*dminNDVI*	*dinfNDVI*	*dmaxNDVI*
Number of plots	120	122	120	122	124	122
RMSE	11.5	16.5	27.5	13.5	8.5	18.0
Bias	2.0	13.5	25.5	−8.5	3.5	15.0
RMSE $_{NULL\ model}$	11.5	11.5	11.5	11	11	11
r*	0.53	0.66	0.56	0.55	0.68	0.57

dminNDVI — date of the beginning of NDVI increase; *dinfNDVI* — date of the inflexion point in the ascendant part of the fitted curve and *dmaxNDVI* — date when NDVI reaches the plateau at the end of the ascendant part of the curve. * All Pearson's coefficients of correlation are statistically significant at 5% probability level.

dminNDVI and 3.5 days using *dinfNDVI* by comparison with *OG10%* and *OG90%* respectively.

The best agreement between predictions and *in situ* observations is obtained between *OG90%* and the inflexion point of the curve (*dinfNDVI*). We also notice that on average measured onset of green-up date *OG90%* is underestimated using *dminNDVI* (negative bias of 8.5 days) and overestimated using *dmaxNDVI* (positive bias of 15 days). *dinfNDVI* constitutes in a way an intermediate marker describing better canopy greenness state during the leaf expansion period.

3.3. Comparison between in situ observations and MODIS MOD12Q2 phenology

As underlined above, MODIS MOD12Q2 products are available only from January 2001. Figs. 5 and 6 show the relationships between *in situ* observations and predictions provided by MODIS MOD12Q2 product during the leaf expansion period. Summary statistics are given in Table 3.

All coefficients of correlation given in Table 3 are statistically significant ($P<0.003$ for the lowest r value) but
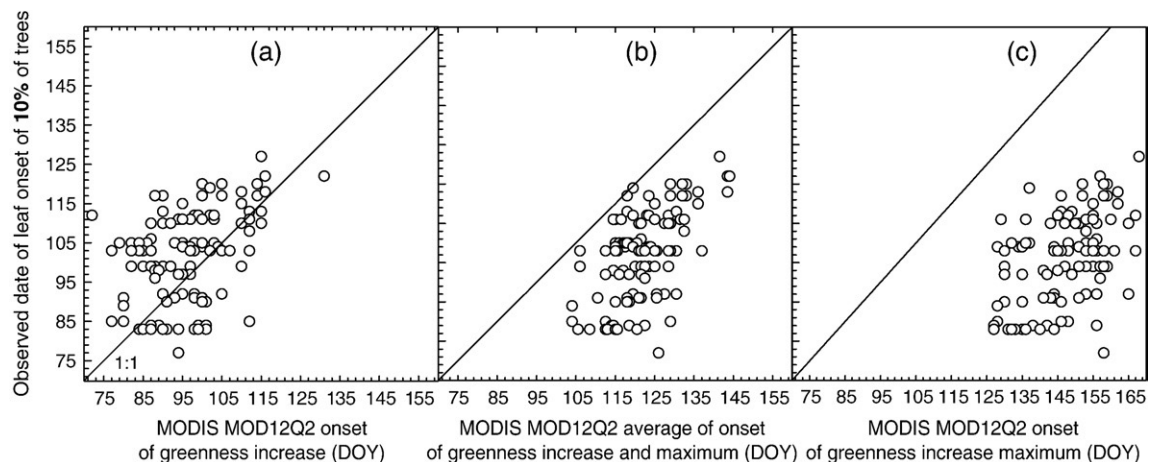

Fig. 5. Comparative analysis between predictions provided by MODIS MOD12Q2 and field observations of the date of onset of green-up at 10% (*OG10%*).
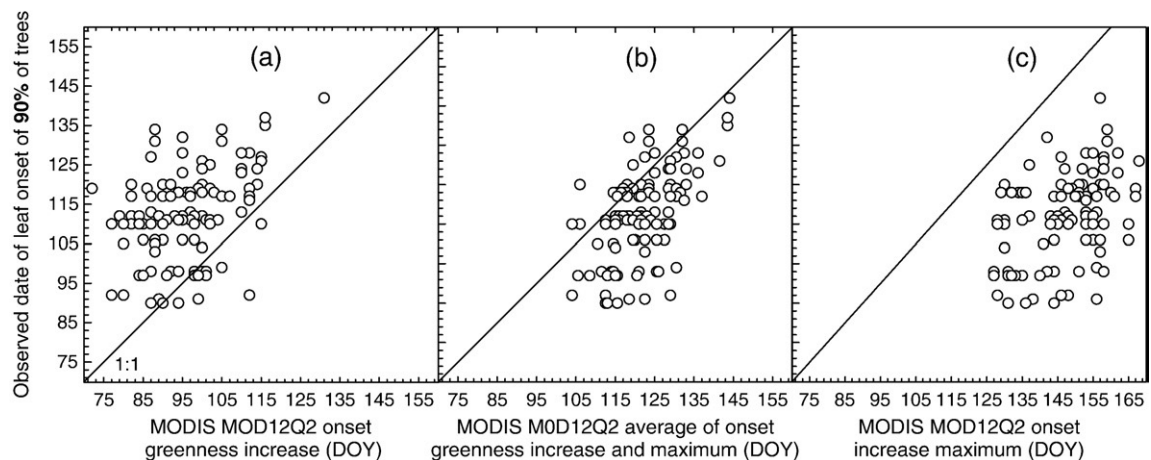

Fig. 6. Comparative analysis between predictions provided by MODIS MOD12Q2 and field observations of the date of onset of green-up at 90% (*OG90%*).

Table 3
Comparative analysis between *in situ* phenological observations *OG10%* and *OG90%* and MODIS MOD12Q2 phenological dates

	With *in situ* onset of green-up *OG10%*			With *in situ* onset of green-up *OG90%*		
	OGI	*(OGI+ OGM)/2*	*OGM*	*OGI*	*(OGI+ OGM)/2*	*OGM*
Number of plots	113	113	113	113	113	113
RMSE	13.5	22.0	47.0	20.5	16.5	36.5
Bias	−6.0	20.0	45.5	−17.0	7.5	34.5
RMSE NULL model	11.5	11.5	11.5	11	11	11
r*	0.40	0.58	0.48	0.39	0.55	0.46

OGI — date of onset of greenness increase; *OGM* — date of onset of greenness maximum and *(OGI+OGM)/2* — the arithmetic average of the two previous dates. * All Pearson's coefficient of correlation are statistically significant at 5% probability level.

Table 4
Average statistics of dates of onset of green-up (day of year) derived from NDVI fits and MODIS MOD12Q2 product against *in situ* observations

Years	Beech plots			Oak plots		
	OG90%	*dinfNDVI*	*(OGI+ OGM)/2*	*OG90%*	*dinfNDVI*	*(OGI+ OGM)/2*
2001	128 (3)	130 (1)	132 (3)	106 (3)	116 (4)	122 (3)
2002	113 (3)	120 (3)	122 (2)	105 (2)	109 (2)	118 (1)
2003	115 (1)	117 (3)	118 (1)	104 (2)	107 (1)	115 (1)
2004	121 (3)	123 (2)	130 (2)	115 (2)	116 (1)	122 (2)

Between brackets () is the standard error of the mean (days).

prediction uncertainties are high. In comparison with *OG10%*, RMSE values are 13.5 days using *OGI* and 47 days using *OGM*. In comparison with *OG90%*, RMSE values are 20.5 days using *OGI* and 36.5 days using *OGM*. For *OG10%* and *OG90%* respectively, bias are negative ([−6, −17 days]) using *OGI* and positive ([45.5, 34.5 days]) using *OGM*.

The quality of predictions in terms of correlation coefficients and uncertainties may be strongly improved if we take the average value of *OGI* and *OGM* as a new marker of onset of green-up date from MOD12Q2 product. By comparison with *OG90%*, RMSE decreases from 20.5 days to 16.5 days and

correlation coefficient increases from 0.39 to 0.55. By comparison with *OG10%*, correlation coefficient increases from 0.4 to 0.58 but RMSE also increases from 13 days to 22 days (Table 3).

3.4. General comparison between in situ observations and MODIS-derived phenological markers

In comparison with the timing of onset of green-up *OG10%*, the best predictions are obtained with the minimum NDVI at the start of growing season in the spring derived from fits of NDVI time-series (*dminNDVI*) and provided by MOD12Q2 product (*OGI*). Uncertainties in predictions assessed by RMSE are close for both markers (*ca* 12.5 days). For both markers, RMSE are higher than RMSE of the null model which means that neither NDVI fits nor MOD12Q2 perform better than the average ground-based dates of onset of green-up.

In comparison with the timing of onset of green-up *OG90%*, phenological dates given by inflexion points (*dinfNDVI*) during the ascending part of the fitted sigmoid curve lead to the best agreement with the *in situ* observations. The best agreement between *in situ* observations and MOD12Q2 phenological dates is also obtained using the average of MOD12Q2 *OGI* and *OGM*. The average makes an improvement of the quality of prediction. Nevertheless, derived MOD12Q2 phenological metrics provided by MOD12Q2 product differ greatly from *in situ* observations and do not perform better than the null model.

Over the four years, temporal variations of observed and predicted phenological dates for the two main species are given in Table 4 and showed in Figs. 7 and 8. Both MOD12Q2 and fitted NDVI time-series give predictions showing the same temporal patterns as the observations. Predictions are overestimated over the four years and for both species. For oak plots, average deviations between predictions and observations ranges between [1.5–10.5 days] using fits and between [6.5–15.5 days] using dates provided by MOD12Q2. For beech plots, average deviations are slightly lower than for oaks,
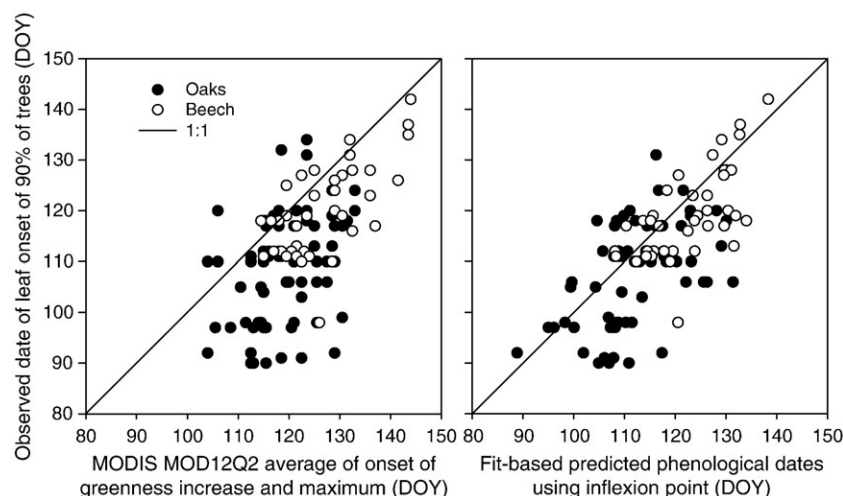

Fig. 7. Comparative analysis between field observations *OG90%* and predictions provided by MOD12Q2 and NDVI time-series for beech and oak plots.
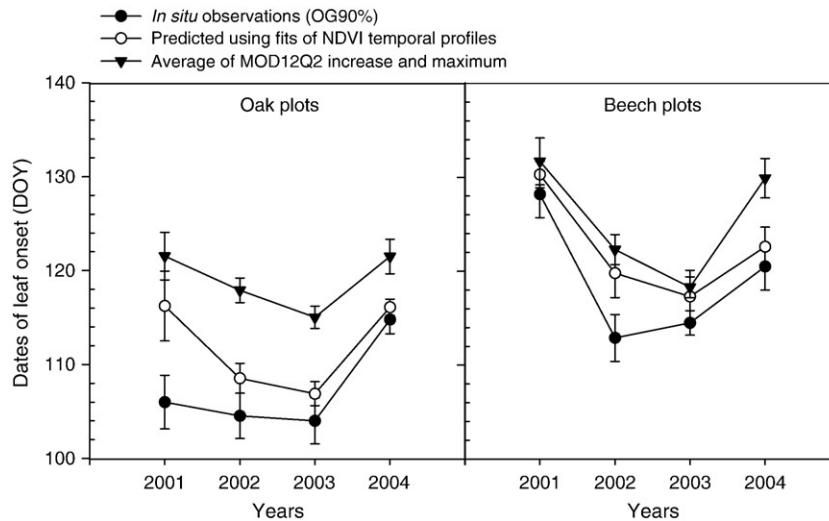
Fig. 8. Average dates of onset of green-up (day of year) derived from NDVI fits and MODIS MOD12Q2 product for beech and oak plots. Vertical bars are ± the standard errors of the mean (days).

between [2–7 days] using fits and between [3.5–9.5 days] using MOD12Q2 products.

4. Discussion

RMSE on predicted leaf onset derived from NDVI time-series using the inflexion point methodology (8.5 days) is of the same order of magnitude than the precision of phenological observations. It is slightly higher compared to locally-fitted bioclimatic models based on temperature sums (in some cases modified by daylength functions) which usually lead to RMSE of 5 days for both beech and oaks species (Kramer et al., 2000; Schaber & Badeck, 2003). But, it is lower than RMSE obtained over temperate biomes through global phenology schemes based on extrapolation of local bioclimatic model to the global scale of about 20 days in Botta et al., 2000. Yet, the availability of climatic data required to force these models may limit their application over large areas.

RMSE values between *in situ* observations and MOD12Q2 phenological dates are of the same order of magnitude than those found in Zhang et al. (2006) between MODIS onset of greenness increase and first and full bloom over many species across Canada. Nevertheless, the timing of flowering is different from the development of green canopy material or "greenness" measured by spectral vegetation indices.

Results also show that the best correlations between predictions and observations are obtained using the *OG90%*. At tree level, *OG10%* and *OG90%* describe the same phenological stage but it is expected that *OG90%* is more representative of phenological stage of the whole plot because *OG10%* is more sensitive to intra-plot genetic variations between trees and to local abiotic conditions. These two dates are also slightly more correlated to the inflexion point derived from modelled NDVI time-series and to the average of the two MOD12Q2 metrics suggesting that these metrics are temporally more stable than NDVI minimum increase and NDVI maximum and capture well inter-site differences in canopy cover at the beginning of

leaf expansion phase. NDVI minimum is expected to be more sensitive to early spring development of vegetation under-story which may lead to an earlier onset of green-up than field observations of overstory phenology as underlined in other studies (Ahl et al., 2006; Fisher et al., 2006). On the contrary, because of saturation problem, NDVI maximum is expected to be less sensitive to differences in phenological responses between sites with dense canopies.

Distinguishing between oaks and beech stands, the predictions are in agreement with *in situ* observations (Figs. 7 and 8). The dates of onset of green-up of these two species are different. For the four years considered, onset of green-up of beech appears later than for oaks (Lebourgeois et al., 2002). On average and over the whole French territory, the onset of green-up of beech is 6 to 14 days later using NDVI fits and 7 to 12 days from *in situ* observations (Fig. 8, Table 4). On the other hand, the length of leaf expansion period estimated using the difference between *dmaxNDVI* and *dminNDVI* is on average 23 days [DOY 100 – 123] for oak stands and 21 days for beech stands [DOY 112 – 133]. These values are in agreement of *in situ* observations as reported in other studies. In European beech stands, the length of leaf expansion period is between 20 to 30 days (Granier et al., 2000; Wang et al., 2005). The same bounds are observed in oak stands (Nizinski and Saugier, 1988). On the contrary, the length of leaf expansion period using MOD12Q2 using the difference between *OGM* and *OGI* is about 50 days for oak [DOY 93 – 143] and 53 [DOY 99 – 152] days for beech. In comparison with NDVI time-series based phenological dates, this overestimation is due to an onset of green-up 7 to 13 days earlier and a leaf maturity about 20 days later. Similar results were reported in other studies. Ahl et al. (2006) observed a length of leaf expansion of 35 days using 16-day MOD43B4 EVI and 17 days from field measurements. In two Carbeuroflux beech stands, Wang et al. (2005) determined the phenological events from MODIS LAI 8-day composite time-series and observed that the onset dates are much earlier than field measurements. On average, the onset dates are 17 and

35 days earlier in both stands. Earlier than observed beginning of spring was also detected through MODIS 8-day FAPAR (Turner et al., 2005; Turner et al., 2006a; Turner et al., 2006b), MODIS 16-day composite EVI, NDVI and MODIS 8-day Gross primary production product (Jenkins et al., 2007). These discrepancies between MODIS composite products and field measurements were partially explained by the inadequacy of the temporal resolution of MODIS composite products to capture rapid changes in canopy structure during the leaf expansion period (Ahl et al., 2006; Schwartz et al., 2002) and/or the effects of understory development (Wang et al., 2005; Turner et al., 2006a). In addition to these effects, remote sensing of spring phenology may be severely affected by snow melting which may artificially increases the NDVI signal and causes erroneously earlier predictions of onset of vegetation (Suzuki et al., 2003; Delbart et al., 2005; Delbart et al., 2006, Kobayashi et al., 2007).

In our study, the effects of vegetation understory on the accuracy of MOD12Q2 estimates of phenological dates can not be excluded particularly in oak stands which may have an understory of hornbeam which shows earlier timing of onset of budburst than oak of about two weeks (unpublished data, see also Wesołowski and Rowiński, 2006). In open canopies, herbaceous species such bramble, brackenfern and purple moor show distinct phenological patterns and usually have earlier onset of green-up than canopy overstory. The effects of snow melting in spring can be excluded. Indeed, during the period 2000–2004, the lowest mean monthly air temperatures were recorded over four beech stands located at high elevations (>1000 m) and ranged between $+0.5°$ and $+4.5$ °C in March and between $+3°$ and $+5.5$ °C in April. Thus, in this study, it seems highly probable that snow melting started several weeks before budburst and had no influence on NDVI based phenological predictions.

The delay of the date of leaf maturity is still more difficult to explain because, as far as we know, there are no species in our study sites which continue their leaf expansion so late in the year. The other factor which influences the agreement between these two methods is the spatial resolution which is of 1 km in MOD12Q2 and 250 m using NDVI time-series. In our study, all plots were chosen in large forest regions. The homogeneity of all plots has been checked visually.

However, these effects can not explain the deviations between MOD12Q2 phenological dates and those derived using NDVI time-series which relate to the same forest stands. This suggests that this discrepancy may be due to a combination of inadequacies of the MODIS products compositing algorithm and the length of compositing (window temporal duration) of monitoring phenological events. Turner et al. (2006a) pointed out that MODIS 8-day LAI and FPAR are maximum values which would tend to anticipate the onset of springtime vegetation but the magnitude of this effect would not be large. Here, we show that using MODIS 16-day EVI, the onset of green-up is 7 to 13 earlier and the date of onset of maturity is also delayed by about 20 days.

The effects of the degradation of the temporal resolution in composite images on the accuracy of prediction of biophysical parameters are obvious (White and Running, 2001). A long compositing period smooths the temporal variability and might not capture the canopy changes over a short-time interval. On the other hand, it increases the probability of having pixel-values not contaminated by clouds. A short compositing period describes more accurately canopy temporal dynamics but the number of spurious pixels resulting from clouds may increases. Using GLOBE budburst measurements (www.globe.gov), White and Running (2001) compared weekly, biweekly and monthly compositing lengths and showed that biweekly compositing length were more appropriate to predict the phenological events. Nevertheless, the authors suggested that these conclusions should be relativized because the quality of field data was not completely guaranteed. Further investigation should be made to clarify the influence of the temporal reso-lution in composite images on the accuracy of phenological transitions dates derived from remote sensing image time-series.

5. Conclusion

Despite the exogenous factors affecting the quality of remote sensing signal particularly sky atmospheric state and cloud cover, MODIS NDVI time-series provide ways for tracking different stages of forest stand growth and development. This study shows that the inflexion point of the curve fitted to MODIS-250 m NDVI temporal profile is a good marker of onset of green-up in deciduous stands. At plot level, the prediction uncertainty is of 8.5 days and the bias is of 3.5 days.

MODIS Global Land Cover Dynamics MOD12Q2 provides estimates of onset of green-up dates which deviate substantially from *in situ* observations and do not perform better than the null model. By comparison with *in situ* observations *OG10%*, RMSE values are 13 days using onset of greenness increase and 47 days using onset greenness maximum. They are 20.5 days and 36.5 days respectively by comparison with *OG90%*. An improvement of prediction quality is obtained if we consider the average of MOD12Q2 onset of greenness increase and max-imum as marker of onset of green-up date. With comparison with *OG90%*, RMSE decreases to 16.5 days.

References

Ahl, D. E., Gower, S. T., Burrows, S. N., Shabanov, N. V., Myneni, R. B., & Knyazikhin, Y. (2006). Monitoring spring canopy phenology of a deciduous broadleaf forest using MODIS. *Remote Sensing of Environment*, *104*, 88−95.

Beck, P. S. A., Atzberger, C., Høgda, K. A., Johansen, B., & Skidmore, A. K. (2006). Improved monitoring of vegetation dynamics at very high latitudes: A new method using MODIS NDVI. *Remote Sensing of Environment*, *100*, 321−334.

Box, J. E., Bromwich, D. H., Veenhuis, B. A., Bai, L. S., Stroeve, J. C., Rogers, J. C., et al. (2006). Greenland Ice Sheet Surface Mass Balance Variability (1988–2004) from Calibrated Polar MM5 Output. *Journal of Climate*, *19*, 2783−2800.

Chen, J., Jonsson, P., Tamura, M., Gu, Z., Matsushita, B., & Eklundh, L. (2004). A simple method for reconstructing a high-quality NDVI time-series data set based on the Savitzky–Golay filter. *Remote Sensing of Environment*, *91*, 332−344.

Chuine, I, Cambon, G., & Comtois, P. (2000). Scaling phenology from the local to the regional level: Advances from species-specific phenological models. *Global Change Biology*, *6*, 943−952.

Chuine, I., Yiou, P., Viovy, N., Seguin, B., Daux, V., & Le Roy Ladurie, E. (2004). Grape ripening as a past climate indicator. *Nature*, *432*, 289−290.

Cihlar, J., Chen, J. M., Li, Z., Huang, F., Latifovic, R., & Dixon, R. (1998). Can interannual land surface signal be discerned in composite AVHRR data? *Journal of Geophysical Research*, *103*, 23163−23172.

Clark, M., & Thompson, R. (2004). Botanical records reveal changing seasons in a warmer world. *Australian Science*, 37−39.

Crucifix, M., Betts, R. A., & Cox, P. M. (2005). Vegetation and climate variability: A GCM modelling study. *Climate Dynamics*, *24*, 457−467.

Delbart, N., Kergoat, L., Le Toan, T., L'Hermitte, J., & Picard, G. (2005). Determination of phenological dates in boreal regions using Normalised Difference Water Index. *Remote Sensing of Environment*, *97*, 26−38.

Delbart, N., Le Toan, T., Kergoat, L., & Fedotova, F. (2006). Remote sensing of spring phenology in boreal regions: A free of snow-effect method using NOAAAVHRR and SPOT-VGT data (1982-2004). *Remote Sensing of Environment*, *101*, 52−62.

Fisher, J. I., Mustard, J. F., & Vadeboncoeur, M. A. (2006). Green leaf phenology at Landsat resolution: Scaling from the field to the satellite. *Remote Sensing of Environment*, *100*, 265−279.

Fisher, J. I., & Mustard, F. (2007). Cross-scalar satellite phenology from ground, Landsat, and MODIS data. *Remote Sensing of Environment*, *109*, 261−273.

Friedl, M. A., Zhang, X., & Tsvetsinskaya, E. (2003). Observing and deriving land cover properties and vegetation dynamics for use in weather and climate models. Session 8. Role of vegetation and land cover/land use in the water cycle. *Symposium on Observing and Understanding the Variability of Water in Weather and Climate. Amer. Meteor. Soc.* Long Beach, CA. Preprints in http://www.ametsoc.org/

Granier, A., Ceschia, E., Damesin, C., Dufrêne, E., Epron, D., Gross, P., et al. (2000). The carbon balance of a young beech forest. *Functional ecology*, *14*, 312−325.

Heidinger, A., Cao, C., & Sullivan, J. (2002). Using Moderate Resolution Imaging spectrometer (MODIS) to calibrate advanced very high resolution radiometer reflectance channels. *Journal of Geophysical Research*. 0148-0227, *107*(D23). doi:10.1029/2001JD002035

Holben, B. N. (1986). Characteristics of maximum-value composite images from temporal AVHRR data. *International Journal of Remote Sensing*, *7*, 1417−1434.

Huete, A., Didan, K., Miura, T., & Rodriguez, E. (2002). Overview of the radiometric and biophysical performance of the MODIS vegetation indices. *Special Issue Remote Sensing of Environment*, *83*, 195−213.

Jenkins, J. P., Braswell, B. H., Frolking, S. E., & Aber, J. D. (2002). Detecting and predicting spatial and interannual patterns of temperate forest springtime phenology in the eastern U.S. *Geophysical Research Letters*, *29*, 54.

Jenkins, J. P., Richardson, A. D., Braswell, B. H., Ollinger, S. V., Hollinger, D. Y., & Smith, M. -L. (2007). Refining light-use efficien cy calculations for a deciduous forest canopy using simultaneous tower-based carbon flux and radiometric measurements. *Agricultural and Forest Meteorology*, *143*, 64−79.

Jönsson, P., & Eklundh, L. (2002). Seasonality extraction by function fitting to time-series of satellite sensor data. *IEEE Transactions on Geoscience and Remote Sensing*, *40*, 1824−1832.

Justice, C., Vermote, E., Townshend, J. R. G., Defries, R., Roy, D. P., Hall, D. K., et al. (1998). The Moderate Resolution Imaging Spectroradiometer

(MODIS): Land remote sensing for global change research. *IEEE Transactions on Geoscience and Remote Sensing*, *36*(4), 1228−1249.

Kaduk, J., & Heimann, M. (1996). A prognostic phenology scheme for global terrestrial carbon cycle models. *Climate Research*, *6*, 1−19.

Kobayashi, H., Suzuki, R., & Kobayashi, S. (2007). Reflectance seasonality and its relation to the canopy leaf area index in an eastern Siberian larch forest: Multi-satellite data and radiative transfer analyses. *Remote Sensing of Environment*, *106*, 238−252.

Kramer, K., Leinonen, I., & Loustau, D. (2000). The importance of phenology for the evaluation of impact of climate change on growth of boreal, temperate and Mediterranean forests ecosystems: An overview. *International Journal of Biometeorology*, *44*, 67−75.

Lebourgeois, F., Differt, J., Granier, A., Bréda, N., & Ulrich, E. (2002). Premières observations phénologiques des peuplements du réseau natioanl de suivi à long terme des écosystèmes forestiers (RENECOFOR). *Revue Forestière Française*, *54*(5), 407−418.

Legates, D. R., & McCabe, G. J. (1999). Evaluating the Use of "Goodness of Fit" Measures in Hydrologic and Hydroclimatic Model Validation. *Water Resources Research*, *35*, 233−241.

Lovell, J. L., Graetz, R. D., & King, E. A. (2003). Compositing AVHRR data for the Australian continent: Seeking best practice. *Canadian Journal of Remote Sensing*, *29*, 770−782.

Ma, M., & Veroustaete, F. (2006). Reconstructing pathfinder AVHRR land NDVI time-series data for the Northwest of China. *Advances in Space Research*, *37*, 835−840.

Menzel, A. (2002). Phenology: Its Importance to the Global Change Community. *Climatic change*, *54*, 379−385.

Myneni, R. B., Keeling, C. D., Tucker, C. J., Asrar, G., & Nemani, R. R. (1997). Increased plant growth in the northern high latitudes for 1981 to 1991. *Nature*, *386*, 698−702.

Moody, A., & Johnson, D. M. (2001). Land-surface phonologies from AVHRR using the discrete Fourier transform. *Remote Sensing of Environment*, *75*, 305−323.

Moulin, S., Kergoat, L., Viovy, N., & Dedieu, G. (1997). Global scale assessment of vegetation phenology using NOAA/AVHRR satellite measurements. *Journal of Climate*, *10*, 1154−1170.

Nash, J. E., & Sutcliffe, J. V. (1970). River flow forecasting through conceptual models part I — A discussion of principles. *Journal of Hydrology*, *10*, 282−290.

Nizinski, J. J., & Saugier, B. (1988). A model of leaf budding and development for a mature Quercus Forest. *Journal of Applied Ecology*, *25*, 643−652.

Reed, B., Brown, J., VanderZee, D., Loveland, T., Merchant, J., & Ohlen, D. (1994). Measuring phenological variability from satellite imagery. *Journal of Vegetation Science*, *5*, 703−714.

Schaber, J., & Badeck, F. -W. (2003). Physiology based phenology models for forest tree species in Germany. *International Journal of Biometeorology*, *47*, 193−201.

Schwartz, M. D. (1990). Detecting the onset of spring: A possible application of phenological models. *Climate Research*, *1*, 23−29.

Schwartz, M. D., Reed, B. R., & White, M. A. (2002). Assessing Satellite-Derived Start-of-Season Measures in the Conterminous USA. *International Journal of Climatology*, *22*, 1793−1805.

Soudani, K., François, C., le Maire, G., Le Dantec, V., & Dufrêne, E. (2006). Comparative analysis of Ikonos, SPOT and ETM+ data for Leaf Area Index estimation in temperate coniferous and deciduous forest stands. *Remote Sensing of Environment*, *102*, 161−175.

Stöckli, R., & Vidale, P. L. (2004). European plant phenology and climate as seen in a 20 year AVHRR land-surface parameter dataset. *International Journal of Remote Sensing*, *25*(17), 3303−3330.

Studer, S., Stöckli, R., Appenzeller, C., & Vidale, P. (2007). A comparative study of satellite and ground-based phenology. *International Journal of Biometeorology*, *51*, 405−414.

Suzuki, R., Tomoyuki, T., & Yasunari, T. (2003). West–east contrast of phenology and climate in northern Asia revealed using a remotely sensed vegetation index. *International Journal of Biometeorology*, *47*, 126−138.

Turner, D. P., Ritts, W. D., Cohen, W. B., Maeirsperger, T. K., Gower, S. T., Kirschbaum, A., et al. (2005). Site-level evaluation of satellite-based global

terrestrial gross primary production and net primary production monitoring. *Global Change Biology*, *11*, 666−684.

Turner, D. P., Ritts, W. D., Cohen, W. B., Gower, S. T., Running, S. W., Zhao, M., et al. (2006a). Evaluation of MODIS NPP and GPP products across multiple biomes. *Remote Sensing of Environment*, *102*, 282−292.

Turner, D. P., Ritts, W. D., Zhao, M., Kurc, S. A., Dunn, A. L., Wofsy, S. C., et al. (2006b). Assessing interannual variation in MODIS-based estimates of gross primary production. *IEEE Transactions in Geosciences and Remote Sensing, 44*, 7, 1899−1907.

Vermote, E. F., & Vermeulen, A. (1999). *MODIS Algorithm Technical Background Document, Atmospheric correction algorithm: Spectral reflectances (MOD09).* NASA contract NAS5-96062.

Viovy, N., Arino, O., & Belward, A. S. (1992). The Best Index Slope Extraction (BISE): A method for reducing noise in NDVI time-series. *International Journal of Remote Sensing*, *13*, 1585−1590.

Zhang, X., Friedl, M. A., Schaaf, C. B., Strahler, A. H., Hodges, J. C. F., Gao, F., et al. (2003). Monitoring vegetation phenology using MODIS. *Remote Sensing of Environment*, *84*, 471−475.

Zhang, X., Friedl, M. A., Schaaf, C. B., Strahler, A. H., & Zhong, L. (2005). Monitoring the response of vegetation phenology to precipitation in Africa by coupling MODIS and TRMM instruments. *Journal of Geophysical Research*, *10*, D12103. doi:10.1029/2004JD005263

Zhang, X., Friedl, M. A., & Schaaf, C. B. (2006). Global vegetation phenology from Moderate Resolution Imaging Spectroradiometer (MODIS): Evaluation of global patterns and comparison with in situ measurements. *Journal of Geophysical Research*, *111*, G04017. doi:10.1029/2006JG000217

Wagenseil, H., & Samimi, C. (2006). Assessing spatio-temporal variations in plant phenology using Fourier analysis on NDVI time-series: Results from a dry savanna environment in Namibia. *International Journal of Remote Sensing*, *27*, 3455−3471.

Wang, Q., Tenhunen, J., Nguyen, Q. D., Reichstein, M., Otieno, D., Granier, A., et al. (2005). Evaluation of seasonal variation of MODIS derived leaf area index at two European deciduous broadleaf forest sites. *Remote Sensing of Environment*, *96*, 475−484.

Wesołowski, T., & Rowiński, P. (2006). Timing of bud burst and tree-leaf development in a multispecies temperate forest. *Forest Ecology and Management*, *237*, 387−393.

White, M. A., Thornton, P. E., & Running, S. W. (1997). A continental phenology model for monitoring vegetation responses to interannual climatic variability. *Global Biogeochemical cycles*, *11*, 217−234.

White, M. A., Schwartz, M. D., & Running, S. W. (1999). Young students, satellites aid understanding of climate-biosphere link. *EOS Transactions*, *81*(1), 5.

White, M. A., & Running, S. W. (2001). Identification of optimal satellite compositing length using GLOBE budburst measurements. *Proceedings of the Sixth Annual GLOBE Conference, Blaine, Washington. GLOBE. July, 2001* (pp. 270−276).

White, M. A., Nemani, R. R., Thornton, P. E., & Running, S. W. (2002). Satellite evidence of phenological differences between urbanized and rural areas of the eastern United States deciduous broadleaf forest. *Ecosystems*, *5*, 260−273.

White, M. A., & Nemani, R. R. (2006). Real-time monitoring and short-term forecasting of land surface phenology. *Remote Sensing of Environment*, *104*, 43−49.

Wolfe, R. E., Roy, D. P., & Vermote, E. (1998). MODIS land data storage, gridding, and compositing methodology: Level 2 grid. *IEEE Transactions on Geoscience and Remote Sensing*, *36*, 1324−1339.

Wolfe, R. E., Nishihama, M., Fleig, A. J., Kuyper, J. A., Roy, D. P., Storey, J. C., et al. (2002). Achieving sub-pixel geolocation accuracy in support of MODIS land science. *Remote Sensing of the Environment*, *83*, 31−49.